JOURNAL OF MATERIALS SCIENCE **35** (2000) 2965–2972

Structure analysis and general characterization of the fluorogallophosphate Mu-2: A new microporous material built from double-four-ring units hosting F^- anions

P. REINERT
Laboratoire de Matériaux Minéraux, ENSCMu., UPRES-A 7016, 3 rue Alfred Werner, 68093 Mulhouse Cedex, France

B. MARLER
Institut für Mineralogie, Ruhr Universität Bochum, D-44780 Bochum, Germany

J. PATARIN
Laboratoire de Matériaux Minéraux, ENSCMu., UPRES-A 7016, 3 rue Alfred Werner, 68093 Mulhouse Cedex, France

A new three-dimensional microporous fluorogallophosphate, named Mu-2, was synthesized from a fluoride-containing aqueous medium in the presence of 4-amino-2,2,6,6-tetramethylpiperidine as organic template. The new material was characterized by microprobe analysis, thermal analysis, X-ray diffraction and solid state NMR spectroscopy. Its structure was determined from X-ray powder as well as single crystal data. The structure of Mu-2 [$Ga_{32}P_{32}O_{120}(OH)_{16}F_8(C_9H_{20}N_2H)_4(C_9H_{20}N_2H_2)_2 \cdot 12H_2O$, $M_r = 6687.0$, cubic, space group I23 (no. 197), $a = 16.3782(2)$ Å, $V = 4393.38(1)$ Å^3, $Z = 1$, $R_F = 7.7\%$ $R_{wp} = 10.7\%$] consists of a cubic arrangement of double-four-ring units (D4R) hosting F^- anions which are interconnected to form a three dimensional but interrupted framework. This arrangement generates a three-dimensional pore system of eight-membered ring channels. Besides the D4R units, two other types of cages are present in the structure occluding the protonated amine and a $(OH)_8$-$(H_2O)_6$-cluster respectively.

1. Introduction

In the eighties a new generation of molecular sieves, $AlPO_4 - n$, based on an aluminophosphate framework were developed [1]. This initial discovery was followed by a number of reports describing partial isomorphous substitutions of aluminum and/or phosphorus by another element such as Si [2], Sn [3], or Me (Me = Mg, Mn, Fe, Co and Zn) [4]. These results proved that new open framework compositions of oxides outside of the known aluminosilicate and silicate zeolites were possible. Since 1985, a large number of gallophosphates with a microporous framework obtained by hydrothermal synthesis were reported in the literature [5–7]. Recently, cobalt-gallophosphates and metal-gallophosphates (metal = Zn, Mn, Co) possessing new microporous framework topologies were obtained by Chippindale *et al.* [8] and Bu *et al.* [9] from quasi non aqueous mixtures. The use of the fluoride method also led to the discovery of a large number of new porous gallophosphates. These materials include for instance the large pore gallophosphate cloverite whose structure displays a three-dimensional 20-membered-ring channel system [10], the LTA-type $GaPO_4$ [11] and several gallophosphates named ULM-*n* [12]. In addition to its mineralizing role the fluoride ion can play a structuring role stabilizing the double-four-ring units (D4R) of a structure. This type of secondary building units had already been observed for the gallophosphate Mu-1 [13], which contains isolated D4R units, the fluorogallophosphate Mu-3 [14] whose structure consists of chains of D4Rs and more recently with the gallophosphates Mu-5 [15] and ULM-18 [16]. The structures of the latter two materials can be described as layers of D4R units. However, in Mu-5, the layers are connected to each other via a gallium-organic complex leading to a three-dimensional inorganic framework. Moreover, F^-trapped into D4R of units had previously been observed for the gallophosphate ULM-5 [17], but in this case F^- is also a component of the framework by bridging gallium atoms.

Here we report the full characterization of a new fluorogallophosphate named Mu-2, which was obtained in an aqueous fluoride-containing medium in the presence of 4-amino-2,2,6,6-tetramethylpiperidine as

organic template. Details of the synthesis of Mu-2 and a brief description of the material was published elsewhere [18].

2. Experimental section

2.1. General characterization of Mu-2

Microprobe analysis (CASTAING-type (CAMEBAX) electron microscope) was performed on large crystals to determine the gallium, phosphorus and fluoride contents of gallophosphate Mu-2.

The analysis of C and N was determined by coulometric and catharometric determinations respectively, after calcination of the samples.

The TG and DSC curves were recorded under air on a Setaram TG/DSC111 thermoanalyser from ambient to 700°C at a heating rate of 5°C min^{-1}. Variable temperature X-ray diffraction (STOE STADI-P diffractometer equipped with a Huber 631 photographic chamber, Cu K_α radiation) was performed under air from 32°C to 752°C in steps of 45°C (time per step = 180 min).

The size and morphology of the crystals were analyzed by scanning electron microscopy using a Philips XL 30 microscope.

The amount of organic species was confirmed by quantitative ^1H liquid nmr spectroscopy. For that, a known amount of the as-synthesized gallophosphate (*ca.* 20 mg) was dissolved into 1 cm^3 of a 6 M HCl solution. Thereafter, 400 mg of a 0.6wt% tetramethylammonium-chloride/D_2O solution were added as an internal standard to the dissolved material. After centrifugation, ≈0.5 cm^3 of the liquid was transferred with an equivalent volume of pure D_2O in a classical glass tube for the NMR analysis. The spectra were recorded on a Bruker AC spectrometer. The recording conditions were: frequency = 250.13 MHz; recycle time = 8 s; pulse width = 2 μs; pulse angle = 30°. The water signal was suppressed with the presaturation technique.

The gallophosphate Mu-2 was characterized by solid state NMR spectroscopy. The ^{13}C CP MAS NMR spectrum and the ^{19}F, ^{31}P, ^{71}Ga NMR spectra were recorded on a Bruker MSL 300 and a Bruker DSX 400 spectrometer respectively. The recording conditions of the CP MAS and MAS spectra are given in Table I.

2.2. Crystal structure determination

For the structure determination several crystals which optically appeared to be single crystals were checked for their quality using the Weissenberg method. While most crystals were unsuitable for single crystal work because of powder-like diffraction patterns a few crystals showed sharp diffraction spots on the Weissenberg photographs. The best crystal (*ca.* 100 μm in diameter) was used to collect 2855 intensities on a four circle Syntex R3 diffractometer in omega/2Θ scan mode. 1014 unique intensities remained after merging the symmetrically related reflections. No absorption correction was made ($\mu = 5.22$ mm^{-1}). Experimental details are listed in Table II. The structure was solved by Direct Methods using the SHELXTL program package [19]. Scattering factors for neutral atoms were used as implemented in the program.

Because of difficulties to interpret the structural features as obtained by the single crystal analysis, X-ray powder diffraction was also applied to this material. As-synthesized Mu-2 crystals were handpicked from the synthesis product to exclude all impurities. The crystals were then ground and sealed in a 0.3 mm capillary. X-ray powder data were collected on a STOE STADI-P powder diffractometer using Cu K_{α_1} radiation in Debye-Scherrer geometry at room temperature. For the Rietveld analysis of the powder data the XRS-82 program system [20] was used. The atomic coordinates of the single crystal structure analysis were taken as a starting model with atomic scattering factors from the International Tables [21]. After subtracting the background, a single peak was selected as standard peak and a peak profile function was calculated. The entire profile was then analyzed for the dependence of the peak width and the peak asymmetry on the diffraction angle. Having done the initial refinements of the profile parameters (2θ zero correction, cell parameters, peak asymmetry and peak width) the structural parameters were refined. Experimental parameters are given in Table II.

TABLE I Recording conditions of the MAS and CP-MAS NMR spectra

	^{19}F	^{13}C	^{71}Ga	^{31}P
Chemical shift reference	$CFCl_3$	TMS	$Ga(H_2O)_6^{3+}$	85% H_3PO_4
Frequency (MHz)	376.5	75.47	112.03	161.98
Pulse width (μs)	2	6.5	0.7	3
Flip angle	$\pi/2$	$\pi/2$	$\pi/12$	$\pi/2$
Contact time (ms)	/	1	/	/
Recycle time (s)	6	5	0.3	8
Spinning rate (Hz)	8000	4000	10000	8000
No. scans	16	600	264800	16

3. Results and discussion

Mu-2 was never obtained as pure phase but crystallized together with variable ratios of two unidentified phases which according to XRD analysis and SEM micrographs are probably layered compounds. Since the crystals of Mu-2 are relatively large, it was possible to eliminate most of the non-desired phases by a repeated ultrasonication and decantation process.

3.1. Crystal morphology and chemical composition

The SEM micrographs reported in Fig. 1a show cubotetrahedral crystals of Mu-2 with a size close to 100 μm. Some crystals are characterized by a smooth surface, whereas others display a rough surface indicating that these "crystals" in fact consist of aggregates of very small crystallites (Fig. 1b). According to the microprobe analysis and the thermal analysis, the as-synthesized samples of Mu-2 have the following composition

(wt%) : Ga : 32.9; P : 13.6; F : 1.73; R : 14.4; H_2O : 5.5

TABLE II Experimental and crystallographic parameters for the structure analysis of Mu-2

	Rietveld refinement	Single crystal analysis
Diffractometer	STOE STADI-P	Syntex R3
Wavelength (Å)	1.5406	0.71073
2Θ range of data collection (°)	7.0–97.0	5.0–60.0
Step size (°2Θ)	0.02	—
No. steps	3790	—
No. contributing reflections	404	820 ($\|F\| > 2\sigma\|F\|$)
No. geometric restraints	32	—
No. structural parameters	40	91
No. profile parameters	2	—
FWHM at 23.0 °2Θ (°2Θ)	0.108	—
R_F	0.077	0.114
R_{wp}	0.107	—
R_{exp}	0.113	—
Program for structure solution	—	SHELX-86
Refinement program	XRS-82	SHELXTL
a (Å)	16.3782(2)	16.377(2)
Unit cell volume (Å^3)	4393.38(1)	4392(1)
Space group	I23	
Unit cell content	$Ga_{32}P_{32}O_{120}(OH)_{16}F_8(C_9H_{20}N_2H)_4(C_9H_{20}N_2H_2)_2\cdot 12H_2O$	
ρ (g/cm^3) (calculated)	2.543	

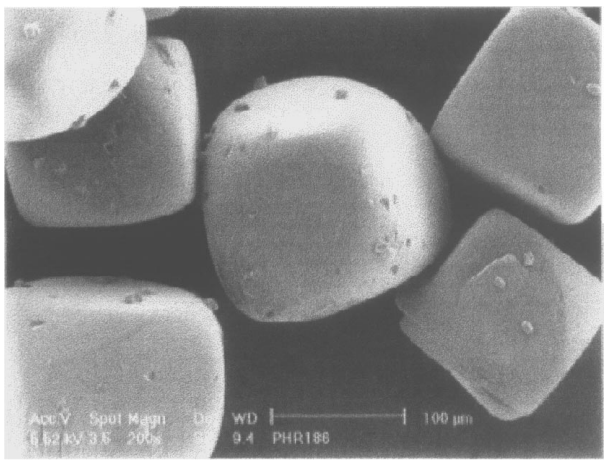

(a)

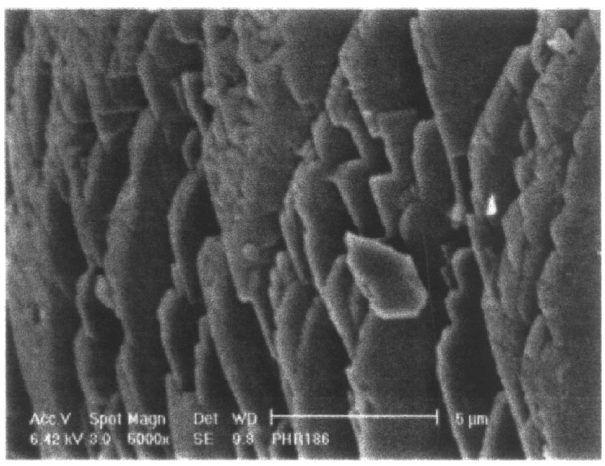

(b)

Figure 1 Scanning electron micrographs of the gallophosphate Mu-2 showing the cubotetrahedral crystals (a), and a detail of the rough surface of some crystals (b).

or

(molar): 34.4 Ga, 32 P, 6.6 F, 6.7 R, 22.3 H_2O

(for comparison normated to 32 P)

The amount of organic species was confirmed by C and N analysis and by quantitative ^{1}H liquid NMR spectroscopy. Based on all analyses including density measurement ($d_{exp} = 2.48(5)$ gcm^{-3}) and the results of the structure determination, the unit cell formula of Mu-2 is:

$$Ga_{32}P_{32}O_{120}(OH)_{16}F_8(C_9H_{20}N_2H)_4(C_9H_{20}N_2H_2)_2 \cdot 12H_2O.$$

Because the amine has to balance the negative charge of the flourine anions, a part of the occluded amine is assumed to be monoprotonated whereas the other part should be diprotonated.

3.2. Crystal structure determination

Optical microscopy showed that all Mu-2 crystals are optically isotropic between crossed nicols proving that Mu-2 has a cubic symmetry. In agreement, the X-ray powder diagram of as-synthesized Mu-2 can unambiguously be indexed with a cubic unit cell. The refinement of the cell parameter led to $a_0 = 16.3782(2)$ Å, and $V = 4393.38(1)$ Å^3. The analysis of the powder pattern as well as the single crystal data revealed systematic extinctions for a body centered cell. No additional extinctions being observed, this led to six possible cubic space groups: I23, I2$_1$3, Im-3, I432, I-43m, Im-3m. Taking into account the morphology of the crystals, all space groups except I23, I2$_1$3 and I-43m can be ruled out since the observed cubotetrahedron (Fig. 1a) is only allowed for crystals having the point group symmetries 23 or -43m.

3.2.1. Single crystal structure analysis

When analyzing the observed diffraction intensities, high or very high internal R values (R_{int}) resulted for the remaining three possible space groups: I23: $R_{int} = 0.092$, I2$_1$3: $R_{int} = 0.092$, I-43m: $R_{int} = 0.236$. Nevertheless, space group I23 was regarded to be the most probable one of this material. The structure could in fact be solved in this space group by direct methods

as implemented in the SHELXTL system. The calculation of the electron density map revealed all Ga and P positions in the asymmetric unit and most of the oxygen positions. These informations clearly showed the general topology of a new microporous $GaPO_4$ framework. The calculation of difference electron density maps revealed the approximate positions of a fluorine atom, a water molecule and electron density maxima in the pore volumes of the structure. Surprisingly, the refinement of the structure model gave a split position for the gallium atom Ga(2). Moreover, the oxygen atom of the hydroxyl group (OH(1)) bonded to Ga(2) remained hidden throughout the refinement. Attempts to refine the structure in space groups $I2_13$ and I-43m gave even less meaningful solutions. Since non-cubic symmetries could be ruled out it was concluded that the single crystal used for the structure determination is twinned with the diffraction spots of the different twin individuals coinciding exactly. The twin law has, so far, not been established. In order to avoid the problems related to the twinning, the structure was finally refined from X-ray powder data.

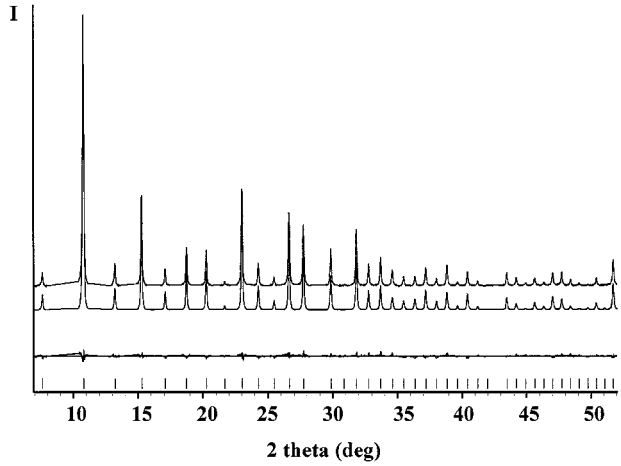

Figure 2 Observed (upper), calculated (middle) and difference (bottom) profiles for the Rietveld refinement of the as-synthesized gallophosphate Mu-2.

3.2.2. Rietveld refinement of the powder data

The structure model of Mu-2, as observed by the single crystal analysis, was used as the starting model, however with the assumption that the Ga(2) position is not split and by adding an oxygen at the OH(1) position which was calculated based on a typical Ga-O bond length. The refinement converged to $R_F = 0.077$ and $R_{WP} = 0.107$ with $R_{exp} = 0.113$) confirming the structure model of Mu-2 as deduced from the single crystal structure analysis. More details of the structure analysis are summarized in Table II. The observed, calculated and difference profiles for the Rietveld refinement are given in Fig. 2. Atomic coordinates, displacement parameters and occupation factors are listed in Table III. Selected bond lengths and angles are reported in Table IV.

3.2.3. Description of the structure

The gallophosphate framework of Mu-2 can completely be built from double-four-ring units (D4R) which are the fundamental building blocks of the structure. Based on the structure refinement all eight D4R's of the unit cell are occupied by a fluoride ion. Each of these $[Ga_4P_4O_{15}(OH)_2F]$ building blocks (Fig. 3) is interconnected with six other building blocks via common oxygen atoms. The remaining two corners of the D4R are T-OH groups (one P-OH and one Ga-OH). The fluorine is off center within the D4R cubes and preferentially linked to three gallium atoms at Ga(1) (Ga(1)-F = 2.24(2) Å). Such a bond length gives rise to a five-fold coordination for this gallium atom with a distorded

TABLE III Atomic coordinates, displacement parameters (U_{iso}) and site occupancy factors (s.o.f.) for Mu-2

Atom	*X*	*Y*	*Z*	s.o.f.	U_{iso} (Å^2)
Ga(1)	0.1132(3)	0.2643(4)	0.7177(3)	1	0.0253(7)[a]
Ga(2)	0.6526(3)	0.6526(3)	0.6526(3)	1	0.0253(7)[a]
P(1)	0.2247(8)	0.2094(7)	0.5827(5)	1	0.0253(7)[a]
P(2)	0.8577(5)	0.8577(5)	0.8577(5)	1	0.0253(7)[a]
F(1)	0.758(1)	0.758(1)	0.758(1)	1.00(2)	0.01(1)
O(1)	0.3122(15)	0.7052(13)	0.5869(6)	1	0.056(2)[b]
O(2)	0.1393(11)	0.2324(17)	0.6141(7)	1	0.056(2)[b]
O(3)	0.0070(4)	0.2812(12)	0.6836(9)	1	0.056(2)[b]
O(4)	0.1335(13)	0.3694(8)	0.7471(19)	1	0.056(2)[b]
O(5)	0.2847(18)	0.2812(17)	0.5893(7)	1	0.056(2)[b]
OH(1)	0.5870(4)	0.5870(4)	0.5870(4)	1	0.056(2)[b]
OH(2)	0.9128(6)	0.9128(6)	0.9128(6)	1	0.056(2)[b]
H_2O	0.00000	0.00000	0.900(1)	0.98(2)	0.066(9)[c]
X(1)	0.00000	0.00000	0.312(2)	1.24[d]	0.066(9)[c]
X(2)	0.398(2)	0.056(2)	0.075(2)	1.24[d]	0.066(9)[c]
X(3)	0.00000	0.552(2)	0.00000	1.24[d]	0.066(9)[c]
X(4)	0.00000	0.895(3)	0.50000	1.24[d]	0.066(9)[c]
X(5)	0.223(3)	0.50000	0.00000	1.24[d]	0.066(9)[c]

[a–c] parameters with the same superscript were constrained to be equal.
[d] *X*(1), *X*(2), *X*(3), *X*(4) and *X*(5) are the five highest peaks in the difference Fourier map. For these positions, the scattering factor of the carbon was used in the refinement. The site occupancy factors of these atoms were fixed at 1.24 to account for the scattering power of the hydrogen atoms of the guest molecule.

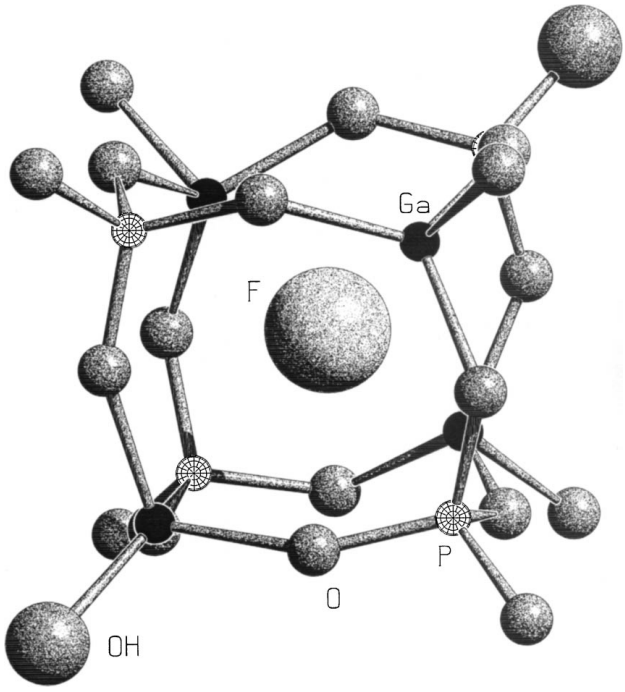

Figure 3 The $[Ga_4P_4O_{15}(OH)_2F]^-$ unit of the Mu-2 structure.

trigonal bipyramidal geometry (see the F-Ga-O angles values (Table IV)). In contrast, the Ga(2) atom which is bonded to the OH(1) group has no additional interaction to the fluorine ion (Ga(2)-F = 3.00(1) Å) and therefore is tetracoordinated to oxygen atoms. Similar to other gallophosphates which contain fluorine in D4R units e.g., $GaPO_4$-LTA [22], the F-P distances are in the range of 2.82(1) to 2.94(2) Å leading to phosphorus atoms with the usual tetrahedral coordination sphere.

The interconnection of the D4R's forms a 3-dimensional but interrupted framework which has a 3-dimensional pore system of 8-MR pore openings (Fig. 4).

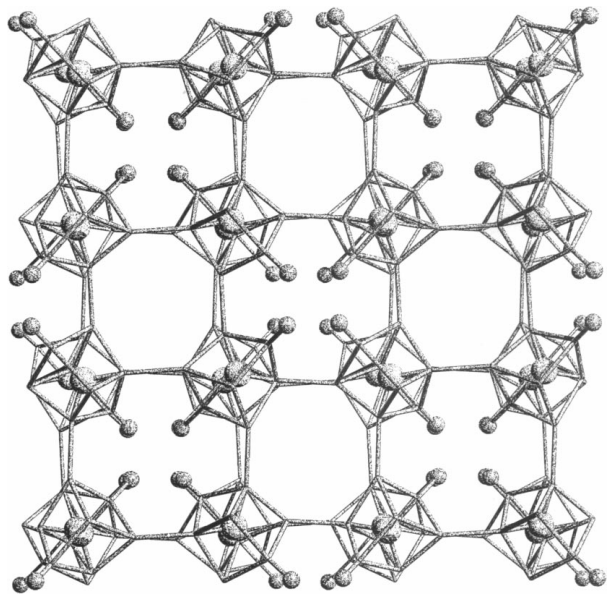

Figure 4 Framework structure of the gallophosphate Mu-2 showing the three types of cages. P and Ga atoms occupy vertices of the network, oxygen atoms, organic species and water molecules are omitted for clarity (large and small spheres represent F^- and OH groups respectively).

TABLE IV Selected bond lengths and angles of the structure of Mu-2. Mean values are given in sharp brackets

a) Gallophosphate framework:

	Distances (Å)		Angles (°)
Ga(1)–O(1)	1.83(2)	O(1)–Ga(1)–O(2)	120(1)
Ga(1)–O(2)	1.83(2)	O(1)–Ga(1)–O(3)	95.1(6)
Ga(1)–O(3)	1.849(9)	O(1)–Ga(1)–O(4)	120(1)
Ga(1)–O(4)	1.82(2)	O(2)–Ga(1)–O(3)	89.0(9)
⟨Ga(1)–O⟩	1.83(1)	O(2)–Ga(1)–O(4)	118(1)
		O(3)–Ga(1)–O(4)	96.3(9)
Ga(2)–O(5)	1.82(2) 3*x*	O(5)–Ga(2)–O(5')	109(1) 3*x*
Ga(2)–OH(1)	1.861(5)	O(5)–Ga(2)–OH(1)	110.0(6) 3*x*
⟨Ga(2)–O⟩	1.83 (2)		
P(1)–O(2)	1.54(2)	O(2)–P(1)–O(3)	109(1)
P(1)–O(3)	1.53(1)	O(2)–P(1)–O(4)	107(1)
P(1)–O(4)	1.54(2)	O(2)–P(1)–O(5)	112(2)
P(1)–O(5)	1.54(3)	O(3)–P(1)–O(4)	107(1)
⟨P(1)–O⟩	1.538(5)	O(3)–P(1)–O(5)	109(1)
		O(4)-P(1)–O(5)	113(2)
P(2)–O(1)	1.56(2) 3*x*	O(1)–P(2)–O(1')	110(1) 3*x*
P(2)–OH(2)	1.565(8)	O(1)–P(2)–OH(2)	108.6(6) 3*x*
⟨P(2)–O⟩	1.561(3)		
		P(2)–O(1)–Ga(1)	130(2)
		P(1)–O(2)–Ga(1)	126(3)
		P(1)–O(3)–Ga(1)	144(3)
		P(1)–O(4)–Ga(1)	135(4)
		P(1)–O(5)–Ga(2)	145(3)
		P–O–Ga	137(9)

b) Fluorine in the D4R:

Atoms	Distances (Å)	Atoms	Angles (°)
F–Ga(1)	2.24(2) 3*x*	F–Ga(1)–O(1)	84.6(4)
F–Ga(2)	3.00(1)	F–Ga(1)–O(2)	90.5(6)
F–P(1)	2.94(2) 3*x*	F–Ga(1)–O(4)	84.6(7)
F–P(2)	2.82(1)	F–Ga(1)–O(3)	178.9(7)
F–O(1)	2.75(1) 3*x*		
F–O(2)	2.90(1) 3*x*		
F–O(4)	2.75(2) 3*x*		
F–O(5)	2.92(2) 3*x*		

c) The water cluster:

Atoms	Distances (Å)
OH(1)–OH(2)	2.85(1) 3*x*
OH(1)–H_2O	2.026(5) 3*x*
OH(2)–OH(1)	2.85(1) 3*x*
OH(2)–H_2O	2.031(7) 3*x*
H_2O–OH(1)	2.026(5) 2*x*
H_2O–OH(2)	2.031(7) 2*x*
H_2O–H_2O	2.33(2) 2*x*
H_2O–H_2O	2.29(3) 2*x*

As expected for a gallophosphate framework there is a strict alternation of the phosphorus and gallium atoms at *T*-sites of the structure. The geometrical analysis of the $GaPO_4$ framework of Mu-2 (Table IV) gave averaged distances of Ga-O = 1.83(1) Å and P-O = 1.54(1) Å, and a mean P-O-Ga angle of 137(9)°. These values are similar to those observed for others porous gallophosphates [10, 17, 22].

The framework of the gallophosphate Mu-2 displays three types of cage-like pores (see Fig. 4):

(i) The first one is the very small D4R unit containing the fluoride anion as described above.

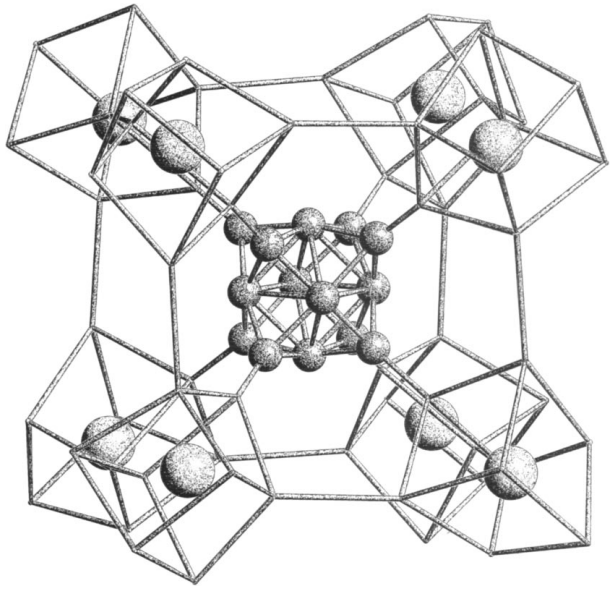

Figure 5 The $(OH)_8$-$(H_2O)_6$-cluster surrounded by eight D4R's which contain F^- anions. ◯ = OH, H_2O; ◯ = F.

(ii) The second cage, noted $[4^65^46^68^2]$, has a free volume of approx. 500 $Å^3$ and is occupied by the 4-amino-2,2,6,6-tetramethylpiperidinium cation (the cation is not shown in Fig. 4). In fact the refined positions of the five highest peaks found in the Fourier map (X(1) to X(5)) do not represent the correct geometry of the occluded template; this is due to positional disorder. The observation that the 4-amino-2,2,6,6-tetramethylpiperidinium guest ion is positionally disordered is in agreement with the fact that the symmetry of the guest (point group symmetry *m*) is incompatible with the symmetry of the $[4^65^46^68^2]$-cage (point group symmetry 222).

(iii) The most interesting feature of this structure type is the $(OH)_8$-$(H_2O)_6$-cluster (Fig. 5) which is located in the third type of "cage" (in Fig. 4 the water molecules are omitted). The T-OH groups of eight D4R's are arranged such that they point to a common center. The OH groups interact with each other by hydrogen bridges with a O-O distance of 2.85(1) Å forming a cube of hydroxyl groups (Fig. 5). This cluster is completed by six water molecules which are located close to the center of the faces of the $(OH)_8$ cube. However the distances for OH-H_2O (O-O = 2.03 Å) and H_2O-H_2O (O-O = 2.30 Å) are abnormally short for hydrogen bonds. Seemingly, it was not possible to determine the exact position of the water molecule from the powder data set which is of somewhat limited quality as indicated by the expected *R*-value $R_{exp} = 0.113$ (see also Table II). The center of the $(OH)_8$-$(H_2O)_6$-cluster, however, is vacant although the void has a free diameter of *ca*. 3 Å which would be large enough to house an additional water molecule for example. Because of the body centered structure of Mu-2 there are two $(OH)_8$-$(H_2O)_6$-cluster per unit cell, one around the origin and one around the center of the unit cell $(\frac{1}{2},\frac{1}{2},\frac{1}{2})$.

3.3. Thermal analysis

The thermal stability of Mu-2 was investigated using high-temperature XRD analysis and TG/DSC analyses.

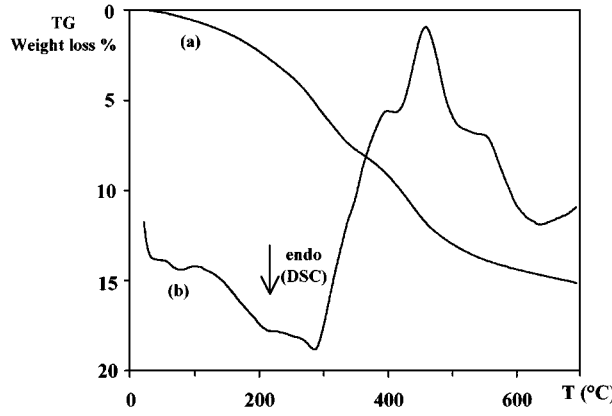

Figure 6 Thermal analysis of Mu-2, (a) TG under air, (b) DSC under air.

A complete amorphization of the structure is observed after heating the as-synthesized sample at 300°C, a cristobalite-type gallophosphate crystallizing at about 600°C. The TG and DSC curves of as-synthesized Mu-2 recorded under air are reported in Fig. 6. Two broad endothermic signals at ∼200 and 300°C are observed. They correspond to the elimination of water molecules of the $(OH)_8$-$(H_2O)_6$-cluster, the dehydroxylation of the T-OH groups (T = Ga, P) and the removal of HF (mass loss: 7.2%). The elimination of these species gives rise to the collapse of the structure. The second loss of 7.9% observed between 340 and 700°C corresponds to a partial removal of the organic species and is characterized by several exothermic peaks on the DSC curve. The sample is black at 700°C indicating that a considerable part of the organic material is still present. A complete expulsion of the organic species was only observed after heating a Mu-2 sample in a different experiment up to 1000°C. In that case the total weight loss was 21.6% (7.2% corresponding to H_2O and HF, 14.4% resulting from the organic species).

3.4. Solid state NMR spectroscopy

3.4.1. ^{13}C CPMAS NMR spectroscopy

The ^{13}C CPMAS NMR spectrum of the as-synthesized Mu-2 is reported in Fig. 7a. It closely resembles the spectrum of the pure 4-amino-2,2,6,6-tetramethylpiperidineamine molecule used as the template in the reaction mixture. The three peaks located at 59.2, 45.2 and 40.7 are assigned to the C(2), C(4) and C(3) atoms of the ring, respectively. The other peaks correspond to the carbon atoms of the four methyl groups. The presence of at least three signals indicate that the four methyl groups of the occluded amine are all symmetrically inequivalent in the crystals structure of MU-2. The organic species in the gallophosphate Mu-2 is assumed to be protonated since the spectrum of MU-2 fits better with the spectrum of the protonated form of the amine (Fig. 7b) than with the one of the non protonated form (Fig. 7c) and because the amine has to balance the charge of the fluorine ions (see chemical composition).

3.4.2. ^{19}F MAS NMR spectroscopy

The ^{19}F MAS NMR spectrum of Mu-2 displays a single line at-72 ppm (Fig. 8). Such a chemical shift was

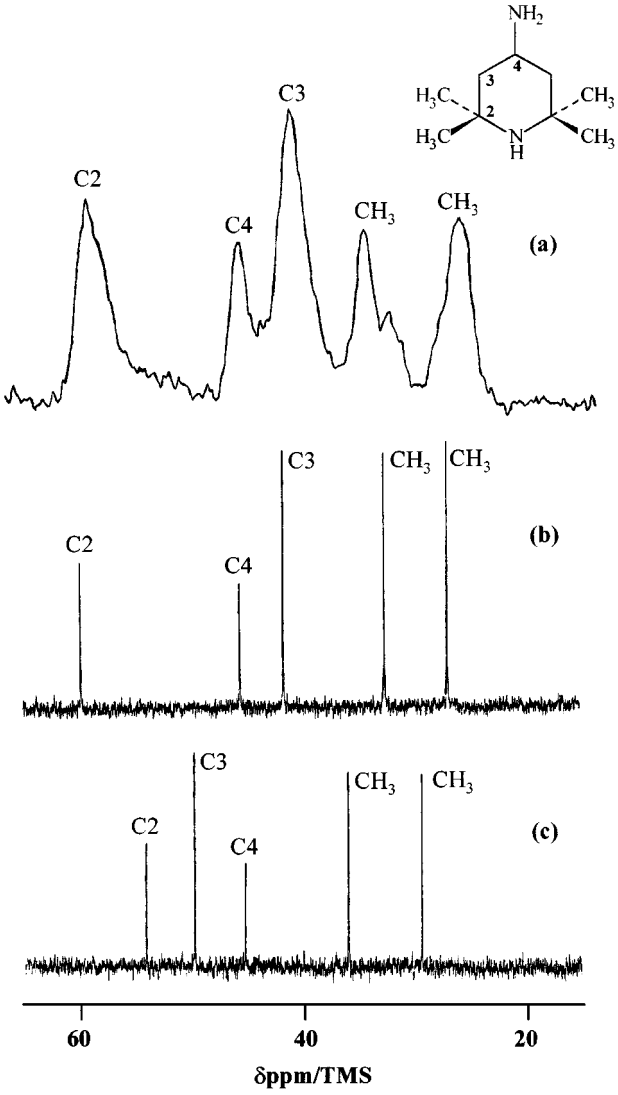

Figure 7 ^{13}C CPMAS NMR spectrum of the gallophosphate Mu-2 (a) and ^{13}C liquid NMR spectra of 4-amino-2,2,6,6-tetramethylpiperidine in neutral (pH∼7), (b) and basic (pH∼12), (c) aqueous solution.

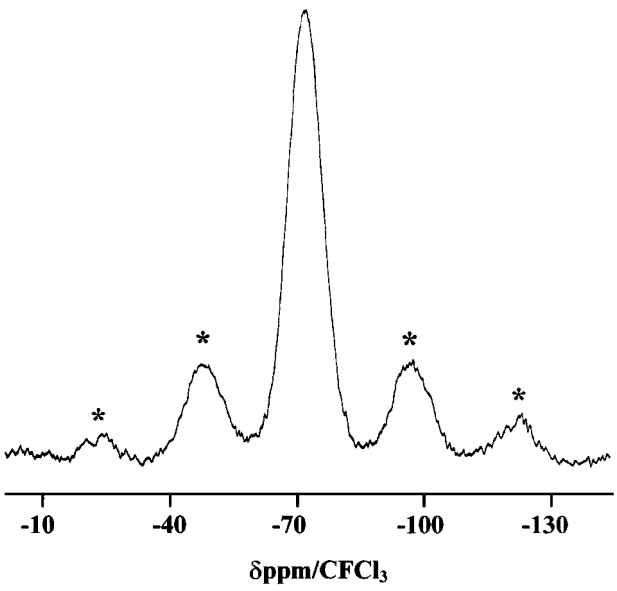

Figure 8 ^{19}F MAS NMR spectrum of the gallophosphate Mu-2 (* = spinning side bands).

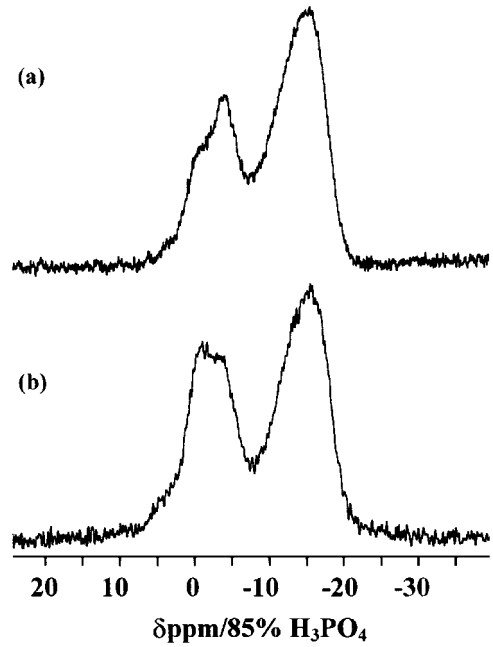

Figure 9 ^{31}P MAS NMR spectra of two different samples of the gallophosphate Mu-2.

previously found for the LTA- and CLO-type gallophosphates and is unambiguously assigned to the fluoride anions trapped in the D4R units of the structure.

3.4.3. ^{31}P MAS NMR spectroscopy

The spectra of two as-synthesized samples of Mu-2 are reported in Fig. 9a and b. These spectra are characterized by the presence of three main components located at −1.1, −3.4 and −15.5 ppm. The signal at −1.1 ppm can be assigned to the presence of an impurity, since the relative intensity of this signal changes from one sample to the other (compare Fig. 9a and b). The intensity ratio of the two other signals ($d = -15.5$ and $d = -3.4$ ppm) is close to 3 and fits well to the expected ratio for the two types of phosphorus sites as obtained by the structure analysis. Therefore, the signal at −3.4 ppm is assigned to phosphorus P(2) (P-OH groups) and the signal at −15.5 ppm to phosphorus P(1) (P(-OGa)$_4$ groups). This was done despite the fact that no significant differences were observed between several ^{1}H-^{31}P CPMAS spectra recorded with different contact times (not reported).

3.4.4. ^{71}Ga MAS NMR spectroscopy

Because of the quadrupolar effect, the ^{71}Ga MAS NMR spectrum of Mu-2 is poorly resolved (Fig. 10). Nevertheless, two types of crystal chemical environments can be distinguished since two main signals are observed at 44 and −74 ppm. According to the chemical shift values and the intensities of these two components, the line at 44 ppm is assigned to the gallium in four-fold coordination (Ga(2)) and the one at −74 ppm to the gallium in five-fold coordination (Ga(1)). Moreover, the baseline shows a broad bump which might be due, as suspected by ^{31}P NMR spectroscopy, to the presence of impurities.

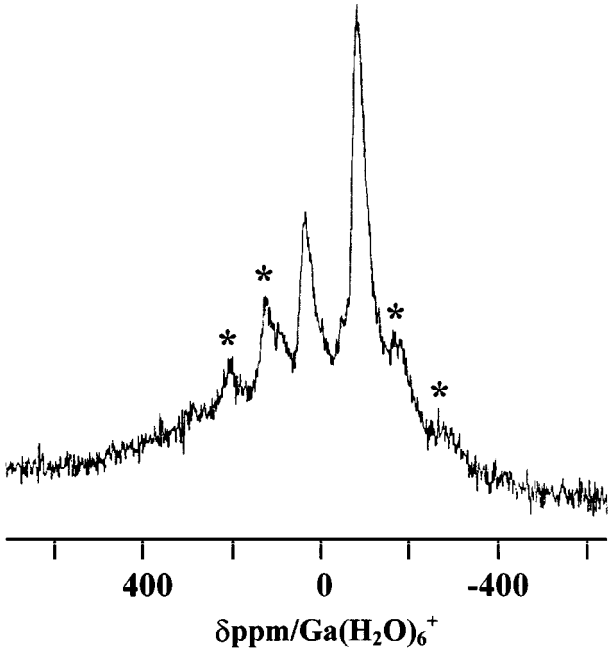

Figure 10 ^{71}Ga NMR spectrum of the gallophosphate Mu-2 (* indicates spinning side bands).

4. Conclusion

The novel hydrated gallophosphate Mu-2 is chemically closely related to Cloverite. Both materials are gallophosphates which have an interrupted framework structure, contain protonated amines as guest ions, water molecules and $[Ga_4P_4O_{15}(OH)_2F]^-$ units. However, the structures of the materials differ considerably. While Cloverite has very large pores, Mu-2 possesses two types of medium size cages with 8-membered-ring openings. The first type of cage (six per unit cell) contains the organic template molecule, whereas the second one (two per unit cell) displays 8 T-OH groups. These OH groups together with six water molecules form a unique OH_8-$(H_2O)_6$-cluster among the gallophosphates.

Acknowledgement

The authors would like to thank IFP for kindly providing the gallium nitrate source, Dr. W. Gebert for collecting the single crystal data and Dr. H. Kessler for fruitful discussions.

References

1. S. T. WILSON, B. M. LOK and E. M. FLANIGEN, US Patent no. 4310440 (1982).
2. B. M. LOK, C. E. MESSINA, R. L. PATTON, R. T. GAJEK, T. R. CANNAN and E. M. J. FLANIGEN, *J. Amer. Chem. Soc.* **106** (1984) 6092.
3. N. J. TAPP and C. M. CARDILE, *Zeolites* **10** (1990) 680.
4. S. T. WILSON and W. C. MERCER, Eur. Patent Appl. 0293920 (1988)
5. J. B. J. PARISE, *Chem. Soc., Chem. Comm.* (1985) 606.
6. S. T. WILSON, N. A. WOODWARD, E. M. FLANIGEN and H. G. EGGERT, Eur. Patent Appl. 0226219 (1987).
7. G. YANG, S. FENG and R. J. XU, *Chem. Soc., Chem. Comm.* (1987) 1254.
8. A. M. CHIPPINDALE and A. R. COWLEY, *Zeolites* **18** (1997) 176.
9. X. BU, P. FENG and G. D. STUCKY, *Science* **278** (1997) 2080.
10. M. ESTERMANN, L. B. MCCUSKER, CH. BAERLOCHER, A. MERROUCHE and H. KESSLER, *Nature* **352** (1991) 320.
11. A. MERROUCHE, J. PATARIN, M. SOULARD, H. KESSLER and D. ANGLEROT, in "Molecular Sieves—Synthesis of Microporous Inorganic Material, Vol. 1," (Van Nostrand Reinhold, New-York, 1992) p. 384.
12. G. J. FÉREY, *Fluorine Chem.* **72** (1995) 187.
13. S. KALLUS, J. PATARIN and B. MARLER, *Microporous Materials* **7** (1996) 89.
14. P. REINERT, J. PATARIN, T. LOISEAU, G. FÉREY and H. KESSLER, *Microporous and Mesoporous Materials* **22** (1998) 43.
15. T. WESSELS, L. B. MCCUSKER, CH. BAERLOCHER, P. REINERT and J. PATARIN, *ibid.*, accepted.
16. F. TAULELLE, A. SAMOSON, T. LOISEAU and G. J. FÉREY, *Phys. Chemistry*, accepted.
17. T. LOISEAU and G. J. FÉREY, *Solid state Chem.* **111** (1994) 407.
18. P. REINERT, B. MARLER and J. PATARIN, *Chem. Commun.* (1998) 1769.
19. SHELXTL Siemens crystallographic Research System, 1990.
20. CH. BAERLOCHER, X-ray Rieteveld System XRS-82, Institut für Kristallographie und Petrologie, ETH, Zürich, 1991.
21. A. J. C. Wilson (ed.), "International Tables for Crystallography, Vol. C," (Kluwer Academic Publishers, Dordrecht, 1995).
22. A. SIMMEN, J. PATARIN and CH. BAERLOCHER, in Proceedings of the 9th Int. Zeolite. Conference., Montreal 1992 (Butterworth-Heineman, Stoneham, 1993) Vol. I, p. 433.

Received 8 July
and accepted 14 December 1999